

COLLIMATOR'S IMPACT INTO THE TRANSVERSE EMITTANCE GROWTH AT KEK COMPACT ERL

O. A. Tanaka[†], N. Nakamura, T. Obina, Y. Tanimoto, T. Miyajima, M. Shimada,
High Energy Accelerator Research Organization (KEK), Tsukuba, Japan

Abstract

In high-intensity particle accelerators, unwanted transverse and longitudinal wakefields arise when the high-charge particle beam passes through the narrow chambers or locations with small transverse apertures, such as collimator jaws. Transverse wakefields impose a transverse kicks to the beam, changing its shape, and leading to the growth of the transverse emittance. Longitudinal wakes cause the beam energy losses, heating of the narrow chambers etc. In the present study we investigated the collimator's impact to the beam. Thus, we evaluated the collimator's wakefields through the CST simulations. We estimated the corresponding transverse kicks and longitudinal wakes. In the summary simulation results were cross-checked with correspondent analytical expressions.

INTRODUCTION

The Compact ERL (cERL) at KEK [1] has five collimators (one in the injector section, one in the merger section and three in the recirculation loop, see Fig. 1) to remove the beam halo and to localize the beam loss. An operation at 10 mA average beam current and 1.3 GHz repetition rate is planned in the near future. The collimator's wakefields are expected to play an important role, even when the bunch charge is increased up to 60 pC. Current beam parameters of the cERL are summarized in the Table 1.

All cERL collimators consist of four cylindrical rods of 7 mm radius made of copper. They could be independently inserted from the top, bottom, left and right sides of the beam chamber. Collimators COL1 – 3 were designed for the straight sections, therefore they have a round chamber 50 mm radius made of stainless steel. Its schematic is given at Fig. 2.a. Note that the energy at collimators COL1 – 2 is 2.9 MeV, while the energy at rest of them is 17.6 MeV. Collimators COL4 – 5 are dedicated to the arc section, thus their chambers are elliptical 70 x 40 mm diameter. Materials used are the same. The detailed scheme can be found at Fig. 2.b.

In the present study, first, we have estimated transverse kicks imposed by the collimator's rods. This calculation is needed to account for the beam blow up (emittance growth) associated with collimator's wake. Then, longitudinal wakes were summarized to obtain the expected energy losses of the beam passing through the collimator and its energy spread. Finally, we have evaluated the same calculations analytically. These results will help us in the beam study, which is planned during the beam operation scheduled in June of this year.

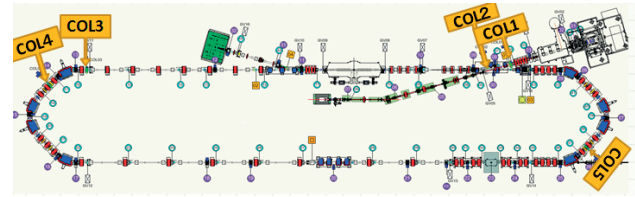


Figure 1: A layout of the cERL and its collimators.

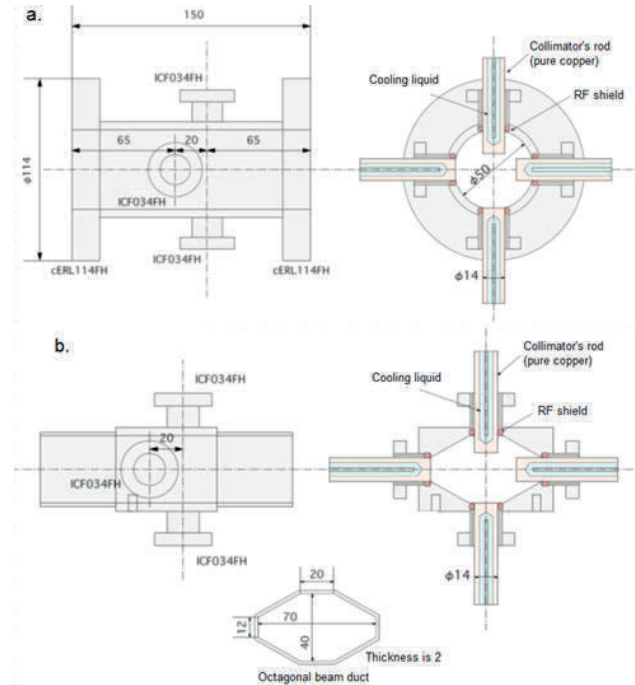


Figure 2: A schematic of the collimators with chambers made of stainless steel and rods made of copper: a. Collimators COL 1 – 3 for the straight sections; b. Collimators COL 4 – 5 for the arc sections.

Table 1: cERL Electron Beam Parameters

Parameter	Design	In operation
Beam energy [MeV]:		
Injector	2.9	2.9
Recirculation loop	18	17.6
Bunch charge [pC]	60	60
Repetition rate [GHz]	1.3	1.3
Bunch length (rms) [ps]	2	Under tuning
Energy spread [%]	0.088	Under tuning
Normalized emittance (rms)		
in injector $\gamma\epsilon_x, \gamma\epsilon_y$ [$\mu\text{m}\cdot\text{rad}$]	1, 1	Under tuning

[†] olga@post.kek.jp.

TRANSVERSE KICKS AND EMITTANCE DILUTION

Let us consider transverse wakefields created by the vertical rods of the collimator. The simplified scheme of the collimator is demonstrated at Fig. 3. Here the vacuum duct's half aperture is $b = 25 \text{ mm}$. The collimator's half gap is $a = [0; 25] \text{ mm}$. There is no tapers, so that the taper angle is $\alpha = \pi/2$. The rod's length is $L = 14 \text{ mm}$. The value y_0 denotes the beam offset. The beam distribution $\lambda(s)$ considered to be a Gaussian.

For the geometry give at Fig. 3 in the beam near-axis approximation, when the dipole kick is applied to the centroid of the bunch, one can write down the dipolar mode of the *geometric component* of the transverse wake kick factor as follows [2]:

$$k_g = \frac{Z_0 c}{4\pi} \left(\frac{1}{a^2} - \frac{1}{b^2} \right) \quad \text{for} \quad \sqrt{\frac{\alpha a}{\sigma_z}} > 0.37. \quad (1)$$

Here we consider the collimator to be in purely diffractive regime [3]. In Eq. (1) the value $Z_0 = 120\pi$ is the impedance of the free space, $c = 2.9979 \times 10^8 \text{ m/s}$ is the speed of light, and $\sigma_z = 0.6 \text{ mm}$ is the rms bunch length.

Then, the *resistive component* of the collimator wake kick factor was evaluated with [4]:

$$k_r = \frac{\pi}{8a^2} \Gamma \left(\frac{1}{4} \right) \sqrt{\frac{2}{\sigma_z \sigma Z_0}} \left(\frac{L}{a} + \frac{1}{\alpha} \right). \quad (2)$$

Note that Eq. (2) is for so-called “long collimator” regime [5] that is exactly our case. Thus, the condition $0.63(2a^2 / Z_0 \sigma)^{1/3} \ll \sigma_z \ll 2a^2 Z_0 \sigma$ is satisfied. The value $\Gamma(1/4) = 3.6265$. And $\sigma = 5.96 \times 10^7 \text{ S/m}$ is the electrical conductivity of copper.

For the wakefields simulation at CST Particle Studio [6], a 3D models listed at Fig.4 a – b were used. We have found the difference in the chamber geometry to be neglected. So, we concentrated on the circular one for simplicity. Six million hexahedral meshes were set for the simulation. The half gap a was scanned from 0.1 mm up to 1.5 mm. The dipolar impact was calculated by setting the integration path to $y = 0$. The quadrupolar impact is calculated by setting the integration path to $y_0 = 0.05 \text{ and } 0.2 \text{ mm}$. A direct integration method was used.

The summary of simulation results together with analytical calculations is demonstrated at Fig. 5. The analytical curve for the geometrical component (blue line) is several orders bigger than those for the resistive-wall component (magenta line). Therefore, the total kick graph (red line) is almost coincides with those for the geometrical component (blue line). Correspondent CST simulation results are given for the beam offset $y_0 = 0.05 \text{ mm}$ (triangles), and for the beam offset $y_0 = 0.2 \text{ mm}$ (circles). Those results are in a good agreement. The resistive-wall component is small due to relatively short length of the collimator (14 mm). And the geometrical component is slightly bigger due to the absence of tapers in the collimator's design.

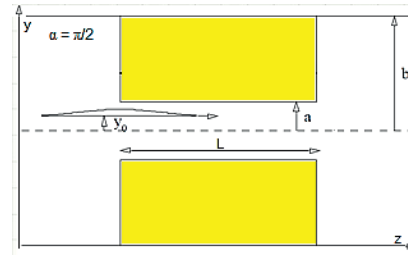


Figure 3: A simplified scheme of the collimator.

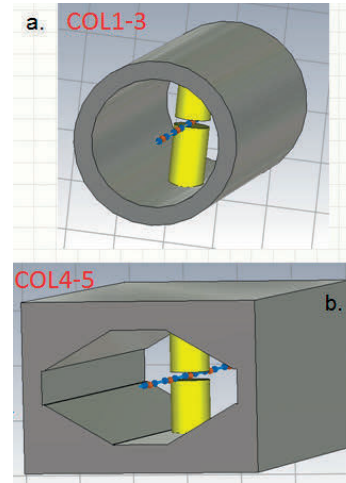


Figure 4: A CST 3D models of the collimators with chambers made of stainless steel and rods made of copper: a. Collimators COL 1 – 3 for the straight sections; b. Collimators COL 4 – 5 for the arc sections.

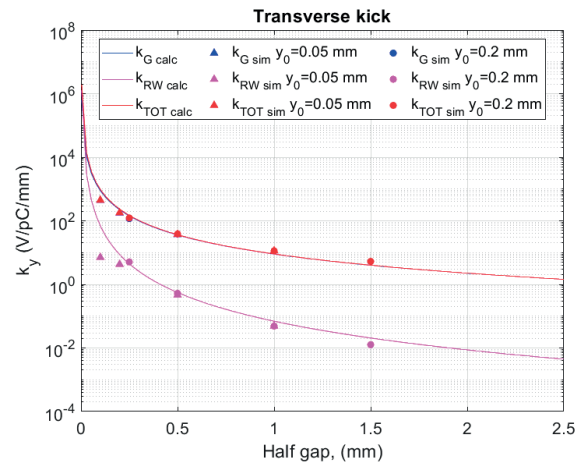


Figure 5: A summary of the transverse wake kick factors of the collimators.

Nevertheless, we have estimated the emittance blow-up for the 60 pC electron bunch at cERL. To account for this effect, the following analytical expression was treated [7]:

$$\frac{\Delta \varepsilon_y}{\varepsilon_{y0}} = \sqrt{1 + \frac{\beta_y \sigma_\omega^2}{\varepsilon_{y0}}}, \quad (3)$$

where the value $\Delta \varepsilon_y$ is the *transverse emittance growth* with respect to the initial emittance ε_{y0} . The rms of the centroid kicks caused by the longitudinally varying field σ_ω could be found as follows [8]:

$$\sigma_{\omega} = \frac{Q}{E/e} k_{\perp}^{rms} y_0. \quad (4)$$

In Eq. (4) the value E is the beam energy at the location of collimator (see Table 1). The value $Q = 60 \text{ pC}$ is a number of electrons per bunch. The value y_0 is the beam centroid offset (see Fig. 3), and lastly, the value k_{\perp}^{rms} is the rms kick factor, estimated for the bunch head-tail difference in kick. For Gaussian bunch $k_{\perp}^{rms} = k_{\perp}/\sqrt{3}$.

Execution results of the Eq. (3) are summarized in Table 2. The values of the initial emittances and beta functions at all locations are design values outputted from the tracking codes (General Particle Tracer [9] for the injector, and Strategic Accelerator Design for the recirculation loop [10]). The value of the transverse kick k_{\perp} is taken with respect to the collimator half gap $a = 1.5 \text{ mm}$, and the beam centroid offsets $y_0 = 0.05 \text{ mm}$ and 0.2 mm . The emittance growth of order one percent or less.

Table 2: Expected Values of the Emittance Blow-Up for the Collimator Half Gap 1.5 Mm

Collimator	Init. emit. [$\mu\text{m}\times\text{rad}$]	Beta func. [m]	Emit. gr. [%]	
			0.05 mm	0.2 mm
COL1 $E = 2.9 \text{ MeV}$	1.15	27.47	0.07	1.07
COL2 $E = 2.9 \text{ MeV}$	1.25	19.23	0.04	0.69
COL3 $E = 17.6 \text{ MeV}$	0.954	34.76	0.02	0.27
COL4 $E = 17.6 \text{ MeV}$	0.954	6.99	< 0.01	0.05
COL5 $E = 17.6 \text{ MeV}$	0.954	6.99	< 0.01	0.05

LONGITUDINAL WAKES AND BEAM ENERGY LOSS

Now, let us consider a problem of wake fields excited by collimators. This problem is important, because the back action of the wakefield from the collimators on the beam leads to an additional energy spread, beam energy losses, and a collimator chamber activation.

The values of the *wake-loss factor* were evaluated numerically through the CST simulation for half-gap values in the range from 0.1 to 1.5 mm. For the analytical description, the following equation was considered [11]:

$$k_{\perp} = \frac{Z_0 c}{2\pi^{3/2} \sigma_z} \ln\left(\frac{b}{a}\right). \quad (5)$$

Eq. (5) is written for the Gaussian bunch distribution and for the “long” collimator in the “diffractive” regime (see Ref. [5] for details). Summary of simulation results (green triangles) and calculations with Eq. (5) (red line) is demonstrated at Fig. 6 below.

Let us estimate the *energy loss per bunch* at one collimator for the bunch charge 60 pC and for the beam – collimator offset 1.5 mm. Following [3] it is expressed as below:

$$\Delta E = k_{\perp} Q^2 = 46.86 \text{ V/pC} \times (60 \text{ pC})^2 = 186.7 \text{ nJ}. \quad (6)$$

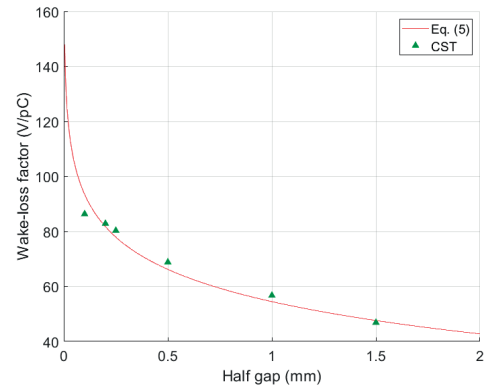


Figure 6: A wake-loss factor vs collimator’s half-gap. The green triangles correspond to the CST simulation results. The red line denotes the analytical calculation.

This energy loss value is suitable for the operation in the burst mode. Then, for the CW mode operation the power loss might be evaluated as $P_{loss} = \Delta E \times f_{rep}$. The value $f_{rep} = 1.3 \text{ GHz}$ in the CW mode, and one can expect the power loss to be 219 W. It is a considerable value, so a water cooling might be required. Then, considering.

Finally, one can easily find the *wake-induced energy spread* for Gaussian bunch due to one collimator. Following [3] and [13] it is might be calculated as 2/5 of the correspondent wake-loss factor. Thus, at a collimator of the half gap 1.5 mm (see Fig. 6) the wake-induced energy spread is expected to be 0.106 % at 17.6 MeV.

CONCLUSION

In the present study we have evaluated the transverse kick and the beam energy loss for the case when the 60 pC electron beam travels near collimator’s rod. The effect of the collimator’s transverse wakefield acting back on beam was found to be negligible due to the collimators geometry. However, it should be taken into account for an intense short bunch, when a considerable beam collimation is required. We have estimated the expected emittance growth due to collimator’s wakefield under current operational conditions at cERL. It is of the order of one percent or less.

Collimators are also generating the wakefield effect that brings an additional energy spread. At cERL we find it to be 0.106 % at 17.6 MeV. Then, we evaluated the energy loss per bunch at one collimator. It is 186.7 nJ for 60 pC bunch. This value is acceptable since the machine is operated in burst mode currently. The CW operation with 219 W power loss might require an additional machine protection.

Considering future cERL upgrade to the IR-FEL [12], a possibility of consequent degradation of the FEL performance should be taken into account. Correspondent power loss was obtained as 13.7 W. In this paper, we have shown numerical and analytical results on the collimator’s wakefields that will be important for the next step operation.

REFERENCES

- [1] T. Obina *et al.*, “1 mA Stable Energy Recovery Beam Operation with Small Beam Emittance”, presented at the 10th International Particle Accelerator Conf. (IPAC’19), Melbourne, Australia, May 2019, paper TUPGW036, this conference.
- [2] G.V. Stupakov, “High-Frequency Impedance of Small-Angle Collimators”, in Proc. of 2001 Particle Accelerator Conf. (PAC01), Chicago, USA, Jun. 2001, pp.1859 – 1861.
- [3] M. Dohlus, I. Zagorodnov, O. Zagorodnova, “Impedances of Collimators in European XFEL”, TESLA-FEL Report 2010-04, July 2010.
- [4] P. Tenenbaum, “Collimator Wakefield Calculations for ILC-TRC Report”, LCCNOTE-0101, 2002.
- [5] I. Zagorodnov and K.L.F. Bane, “Wakefield calculations for 3D collimators”, in *Proc. of 10th European Particle Accelerator Conference (EPAC 2006)*, Edinburgh, UK, June. 2006, pp. 2859 – 2861.
- [6] CST-Computer Simulation Technology, CST PARTICLE STUDIO,
<http://www.cst.com/Content/Products/PS/Overview.aspx>
- [7] M. Dohlus, T. Limberg, “Impact of Optics on CSR-Related Emittance Growth in Bunch Compressor Chicanes”, in *Proc. of 21st Particle Accelerator Conference (PAC05)*, Knoxville, USA, May 2005, paper TPAT006, pp. 1015-1017.
- [8] S. Di Mitri, PhysRevSTAB 13,052801 (2010).
- [9] GPT - A simulation tool for the design of accelerators and beam lines, <http://www.pulsar.nl/gp>
- [10] Strategic accelerator design, <http://acc-physics.kek.jp/SAD>
- [11] S. Heifets and S. Kheifets, “Coupling impedance in modern accelerators”, Rev Mod Phys 63, 631 (1991).
- [12] R. Kato, N. Nakamura, H. Sakai, M. Shimada, K. Tsuchiya, “cERL Upgrade Plan for an IR FEL”, presented at the 10th International Particle Accelerator Conf. (IPAC’19), Melbourne, Australia, May 2019, paper TUPRB107, this conference.
- [13] A. Brynes, G. Castorina, O. Frasciello, A. Marcelli, B. Spataro, “Studies of geometric wakefields and impedances due to collimators”, INFN Report INFN-16-10/LNF, June 2016.